Zonal-Flow Dynamics and Size Scaling of Anomalous Transport

Liu Chen
Department of Physics and Astronomy, University of California, Irvine, California 92717-4575, USA

Roscoe B. White
Princeton Plasma Physics Laboratory, P.O. Box 451, Princeton, New Jersey 08543, USA

F. Zonca
Associazione Euratom-ENEA sulla Fusione, C.R. Frascati, C.P. 65-00044 Frascati, Italy
(Received 24 July 2003; published 20 February 2004)

Nonlinear equations for the slow space-time evolution of the radial drift-wave envelope and zonal flow amplitude have been self-consistently derived for a model nonuniform tokamak equilibrium within the coherent four-wave drift wave-zonal flow modulation interaction model of Chen, Lin, and White [Phys. Plasmas **7**, 3129 (2000)]. Solutions clearly demonstrate turbulence spreading due to nonlinearly enhanced dispersiveness and, consequently, the device-size dependence of the saturated wave intensities and transport coefficients.

DOI: 10.1103/PhysRevLett.92.075004 PACS numbers: 52.55.Dy, 52.55.Fa, 52.55.Tn

The dependence of plasma confinement on the device size is obviously a very crucial issue in fusion energy research. Heuristic estimates of transport coefficients, based on random walk arguments [1], are commonly used and yield Bohm-like transport, $\chi \propto \chi_B = (cT/eB)$, when the step size is taken to have macroscopic scaling and the time step is estimated with the inverse linear growth rate. Meanwhile, diffusion coefficients are expected to scale as gyro-Bohm, $\chi \propto \chi_{GB} = \rho_* \chi_B$, when the step size is assumed to be microscopic. Here $\rho_* = \rho_i/L_p$ with ρ_i and L_p being, respectively, the ion Larmor radius and the plasma inhomogeneity scale length. However, recent experimental evidence of Bohm-like transport was obtained on the Joint European Torus [2] as well as on DIII-D [3], even for microscopic scaling of plasma turbulence. This fact clearly demonstrates the validity limits of random walk estimates of plasma transport and, at the same time, provides a challenging problem to plasma theory which has recently received increasing attention (see, e.g., Ref. [4] and references therein). At present, however, most of the analyses are based on massive numerical simulations, except in a few cases [5,6]. The need for more fundamental theoretical investigations of transport size scaling is the main motivation for this work.

Assuming drift waves are responsible for the anomalous transport, size scaling can be reduced, in the simplest model, to the dependence of drift-wave fluctuation intensity on ρ_*. The coherent four-wave drift wave-zonal flow modulation interaction model of Chen, Lin, and White [7] has captured the essential features observed in global gyrokinetic simulations in the $\rho_i/L_p \to 0$ limit. We are thus motivated to adopt the same model as a theoretical paradigm, including finite L_p (i.e., finite ρ_*) plasma inhomogeneities. In this finite-ρ_* coherent four-wave model, not only the drift-wave (pump) radial envelope will be localized, leading to reduction in the modulational instability growth rate due to the finite interaction region, but more interestingly the damped pump and sidebands will disperse outward leading to radial spreading of the drift-wave turbulence, qualitatively similar to that observed in recent simulations [4]. As we show in the following, this turbulence characteristic behavior crucially depends on the wave dispersive properties of the radial envelope, which, in turn, depend intrinsically on the toroidal geometry of the considered system. As a consequence, the model we propose here predicts that numerical simulations of turbulent transport in cylindrical plasmas should be generally and profoundly different from those in a torus.

Following the theoretical formalism introduced in Refs. [7,8], we assume that fluctuating fields are given by a single $n \neq 0$ drift wave, $\delta\phi_d$, and a zonal ($n = m = 0$) scalar field perturbation $\delta\phi_z$:

$$\begin{aligned} \delta\phi_d &= \delta\phi_0 + \delta\phi_+ + \delta\phi_-, \\ \delta\phi_0 &= e^{in\varphi} \sum_m A_{0,m} e^{-im\vartheta} \phi_0(nq - m, r) + \text{c.c.}, \\ \delta\phi_\pm &= e^{\pm in\varphi} \sum_m A_{\pm,m} e^{\mp im\vartheta} \phi_\pm(nq - m, r) + \text{c.c.}, \\ \delta\phi_z &= A_z(r) + \text{c.c.}, \end{aligned} \tag{1}$$

where m and n are, respectively, poloidal and toroidal mode numbers. To simplify notations, time dependencies are suppressed, while (r, ϑ, φ) denote a right-handed toroidal coordinate system and q is the tokamak safety factor. Equations (1) explicitly indicate the existence of two characteristic spatial scales for high-n drift waves [9]. The long scale reflects the characteristic radial variation of A_0, $A_\pm$, A_z, i.e., of mode envelopes and zonal flow, and is typically shorter than the equilibrium scale L_p. The short radial scale, instead, is associated with the parallel

(to the ambient magnetic field) mode structure. It is $\approx n^{-1}dr/dq$ and can be formally separated via the Fourier transform [9]

$$\phi_{0,\pm}(nq-m,r)=\int_{-\infty}^{\infty}\frac{d\theta}{\sqrt{2\pi}}e^{-i(nq-m)\theta}\psi_{0,\pm}(\theta,r), \quad (2)$$

where r dependencies reflect slow residual radial variations on the equilibrium scale.

The typical time for wetting the parallel mode structure is $O(\omega^{-1})$, the inverse mode frequency. Zonal flows, meanwhile, have characteristic times that are long compared with ω^{-1} and typically of $O(\gamma_L^{-1})$, the inverse drift-wave growth rate. Assuming formal proximity to marginal stability such that $\gamma_L \ll |\omega|$, nonlinear dynamics, thus, affects only radial envelope and zonal flow structures, leaving parallel mode structures essentially unchanged. That is, radial envelope and zonal flow structures could be completely different from those predicted by linear theory and need to be determined consistently from nonlinear equations for their slow space-time evolution. Detailed derivations of these equations will be given elsewhere [6]. The basic approach for such derivations, however, can be found in Refs. [7,8] in the $k_\perp^2\rho_i^2 \ll 1$ limit, $k_\perp$ being the perpendicular (to the ambient magnetic field) drift-wave vector. These equations are the quasineutrality conditions for the fluctuating fields of Eq. (1); explicitly written in a closed form via direct solution of the nonlinear gyrokinetic equation [10]. This nonlinear system of partial differential equations (2D in space plus time) can then be reduced to a nonlinear system of pseudodifferential equations (1D in space plus time) based on time and spatial scale separation of the mode structures; i.e., $\gamma_L \ll |\omega|$ and $|n^{-1}dr/dq| \ll \Delta$, Δ being the characteristic width of the radial envelope and zonal flow structures. The parallel mode structures $\psi_0(\theta,r)$, $\psi_\pm(\theta,r)$ are, thus, given by the linear theory, and one may adopt eikonal ansatz for radial envelopes

$$\begin{aligned} A_{0,m} &= A_0(r) = e^{i\int n\theta_k dq},\\ A^*_{-,m} &= A_{+,m} = A_+(r) = e^{i\int n\theta_k dq}(e^{i\int n\theta_{kz}dq} + \text{c.c.}),\\ A_z &= e^{i\int n\theta_{kz}dq} + \text{c.c.} \end{aligned} \quad (3)$$

Note, in Eqs. (3), we take $k_z \approx k_r$, and assume $|\partial_r k_r/k_r^2| \ll 1$ and $|\partial_r k_z/k_z^2| \ll 1$ for consistency. Here, $k_z^{-1} = \theta_{kz}^{-1}n^{-1}dr/dq$ and $k_r^{-1} = \theta_k^{-1}n^{-1}dr/dq$, $2\pi k_z^{-1}(k_r^{-1})$ are the characteristic wavelengths of zonal flow (drift-wave) oscillations. Within this framework, one can field line average the quasineutrality conditions for drift-wave and zonal flow and reduce them to the following standard form for $k_\perp^2\rho_i^2 \ll 1$ [6–8]:

$$\begin{aligned} \mathcal{L}_P P &= 2S\partial_x Z, \qquad \mathcal{L}_S S = -P\partial_x Z,\\ \mathcal{L}_Z Z &= 2\mathrm{Re}[P^*\partial_x S - S\partial_x P^*]. \end{aligned} \quad (4)$$

Note that Eqs. (4) have the Reynolds-stress-like antisymmetric nonlinearity, as expected for electrostatic drift waves in the $k_\perp^2\rho_i^2 \ll 1$ limit [10,11]. The linear operators $\mathcal{L}_P$, $\mathcal{L}_S$, $\mathcal{L}_Z$, meanwhile, are defined in terms of the local drift-wave dielectric function $D = D_R(r,\omega,\theta_k) + iD_I(r,\omega,\theta_k)$, with the wave frequency ω_0 and envelope radial wave number $\theta_{k0}(r)$ given by $D_R(r,\omega_0,\theta_{k0}(r)) = 0$. More precisely,

$$\begin{aligned} \mathcal{L}_{P,S} &= \partial_\tau - \bar{\gamma}_{P,S} - 2\delta^{1/2}\partial_x + i\Gamma(\lambda+\xi) + i\partial_x^2,\\ \mathcal{L}_Z &= (\partial_\tau + \bar{\gamma}_z), \end{aligned} \quad (5)$$

where $\Gamma = \omega/|\gamma_{LP}(x=\infty)|$ is the mode frequency normalized to the drift-wave growth rate, time is normalized as $\tau = |\gamma_{LP}(x=\infty)|t$, $[\bar{\gamma}_{P,S}, \bar{\gamma}_z] = [\gamma_{LP,S}, \nu_z]/|\gamma_{LP}(x=\infty)|$, ν_z being the zonal flow collisional damping, $\nu_z \approx (1.5\epsilon\tau_{ii})^{-1}$ [12], with $\epsilon = r/R_0$ and R_0 the tokamak major radius. Equations (5) include the leading order relevant physical effects on the radial wave-packet propagation along the linear characteristics, i.e., drive or damping, group velocity, potential well, and focusing or defocusing, respectively [6]. Here, the normalized fields P, S, Z are related with A_0, A_+, A_z as

$$\begin{aligned} \frac{e[A_0,A_+]}{T_e} &= \Lambda\left(\frac{1.6q^2}{\alpha_0\epsilon^{1/2}}\omega_0\frac{\partial D_R}{\partial\omega_0}\frac{T_i}{T_e}\right)^{1/2}\frac{[P,-iS]}{s\Gamma^{1/2}},\\ \frac{eA_z}{T_e} &= \Lambda\left(\omega_0\frac{\partial D_R}{\partial\omega_0}\right)\frac{Z}{s\Gamma^{1/2}}, \end{aligned} \quad (6)$$

where $\Lambda = (\omega_0/\omega_{ci})(r/nq\rho_i)^2(\lambda^{1/2}/\theta_{k0})$, $s = d\ln q/d\ln r$, $\alpha_0 = 1 + \delta p_{\perp i}/(en_0\delta\phi)$ [7], $\delta p_{\perp i}$ is the perpendicular ion pressure fluctuation, n_0 is the equilibrium density, and other notations are standard. The normalized radial coordinate x and the other quantities to be defined in Eqs. (5) and (6) are given by

$$\begin{aligned} \xi &= \frac{\theta_{k0}\partial D_R/\partial\theta_{k0} - \theta_{k0}^2\partial^2 D_R/\partial\theta_{k0}^2}{\omega_0\partial D_R/\partial\omega_0},\\ \lambda &= \frac{\theta_{k0}^2}{2}\frac{\partial^2 D_R/\partial\theta_{k0}^2}{\omega_0\partial D_R/\partial\omega_0}; \qquad \delta^{1/2} = \frac{\xi\Gamma^{1/2}}{2\lambda^{1/2}},\\ \gamma_L &= -\frac{D_I}{\partial D_R/\partial\omega_0}; \qquad \frac{\partial}{\partial x} = \frac{\lambda^{1/2}\Gamma^{1/2}}{\theta_{k0}n(dq/dr)}\frac{\partial}{\partial r}. \end{aligned} \quad (7)$$

In the cylindrical limit, $\partial D_R/\partial\theta_{k0} = 0$ and $\xi = \lambda = \delta^{1/2} = 0$ as well as $\partial_x = 0$ in Eqs. (5) and (7), demonstrating the crucial importance of toroidal geometry.

Equations (4) generally require numerical solutions. As a simple but relevant paradigm, we take Gaussian nonuniformity profiles and quadratic dispersiveness for numerical studies of Eqs. (4). That is, $D_R = \omega/\omega_0 - 1 + \theta_k^2 + V(x)$, with the potential well $V(x) = 1 - \exp(-x^2/L^2)$, where L is related with the equilibrium profile scale as $L = |ndq/dr|L_p/\Gamma^{1/2}$. We also choose $D_I = -(\bar{\gamma}_P(x)/\Gamma) = -(1/\Gamma)[A\exp(-x^2/L^2) - 1]$ for the pump and $D_I = (\bar{\gamma}_d/\Gamma)$ for the sidebands such that

$$\mathcal{L}_P = \partial_\tau - \bar{\gamma}_P(x) = i\Gamma V(x) + i\partial_x^2,$$
$$\mathcal{L}_S = \partial_r + \bar{\gamma}_d - i\Gamma V(x) + i\partial_x^2, \qquad \mathcal{L}_Z = (\partial_r + \bar{\gamma}_z). \tag{8}$$

From Eqs. (4) and (8), we readily recover the local limit considered in Ref. [7] by taking $L \to \infty$, $P = P_0(t)$, $S = S_0(t)\cos(\kappa_z x)$, and $Z = Z_0(t)\sin(\kappa_z x)$. In that case, maximum zonal flow growth rate for fixed pump amplitude, $\Gamma_{z,\max} = |P_0|^2 - \bar{\gamma}_z$, is expected for $\kappa_z^2 = \bar{\gamma}_d + \Gamma_{z,\max}$, i.e., for $\theta_{kz} = \Gamma^{-1/2}(\bar{\gamma}_d + \Gamma_{z,\max})^{1/2}$ [7].

Fast radial nonlinear oscillations of sidebands and zonal flow on the characteristic scale $\approx \kappa_z^{-1}$ are a general feature of the solutions of Eqs. (4) also for finite L [6]. The spatially averaged drift-wave intensity on this short scale is $\bar{I} = \overline{|P + 2S|^2} = |P_0|^2 + 2|S_0|^2$ and, for the fixed point solution as $L \to \infty$, $\bar{I}_f = |P_{0,f}|^2 + 2|S_{0,f}|^2 = \bar{\gamma}_z(\bar{\gamma}_d + 2\bar{\gamma}_{P0})|\bar{\gamma}_d - \bar{\gamma}_{P0}|^{-1}$, with $\bar{\gamma}_{P0} = A - 1$. Assuming drift waves are responsible for anomalous transport and that anomalous diffusion in an infinite system has gyro-Bohm scaling, $\chi_\infty = \chi_{\rm GB} \approx \rho_* \omega_{ci} \rho_i^2$, the present model yields $\chi = \chi_{\rm GB}(\bar{I}/\bar{I}_f)$. Thus, any size scaling of anomalous transport can be reduced to the dependence of $\bar{I}$ on L, and ultimately on ρ_*. In order to investigate this aspect, we have solved Eqs. (4) and (8) numerically, keeping $\bar{\gamma}_z = 0.1$, $\bar{\gamma}_d = 1$, and $\Gamma = 4$ fixed, while changing both $\bar{\gamma}_{P0} = A - 1$ and L to assess $\bar{I}$ dependencies on these parameters. Snapshots of simulation results for the wave fields at different times are shown in Fig. 1 for $A = 1.15$ and $L = 200$. They clearly demonstrate outward radial dispersion of pump, assisted by the nonlinear modulation interaction and leading to radial spreading of the drift-wave turbulence qualitatively similar to that observed in recent simulations by Lin *et al.* [4]. Pump radial spreading is then followed by similar spreading of zonal flow and sidebands, as indicated in Fig. 2. Numerical solutions can be understood via asymptotic analyses of Eqs. (4) and (8), employing the optimal ordering $\partial_\tau \approx \bar{\gamma}_z \approx \bar{\gamma}_{P0} \ll \bar{\gamma}_d$. Here, we omit the details and report only some of the main results [6]. The leading order solution can be represented as $P \sim P_0(x_1, \tau)$, $S \sim S_0(x_2, \tau)\cos(\kappa_z x)$, $Z \sim Z_0(x_2, \tau)\sin(\kappa_z x)$, $x_1 \approx L^{1/2}$, $x_2 \approx L^{1/4}$, with $\kappa_z = \bar{\gamma}_d^{1/2}$ for the fastest growing zonal flow. Equations (4) and (8) then reduce to $S_0 = -(1 + i)P_0 Z_0/2\bar{\gamma}_d^{1/2}$,

$$[\partial_\tau - \bar{\gamma}_P(x) + Z_0^2/2 - i\Gamma V(x) + iZ_0^2/2 + i\partial_x^2]P_0 = 0,$$
$$[\partial_\tau + \bar{\gamma}_z - |P_0|^2 - 2\bar{\gamma}_d^{-1}|P_0|^2\partial_x^2]Z_0 = 0. \tag{9}$$

Zonal flows, thus, act both as nonlinear damping as well as antipotential well on the drift-wave pump. Meanwhile, the pump drives zonal flows nonlinearly, but it induces nonlinear diffusion as well. Thus, zonal flows are generated via modulational instability and expel the pump, explaining causality in the temporal sequence of Fig. 2, which manifests itself in numerical simulations as turbulence spreading [4,5]. When radial spreading stops and the fluctuation intensity has reached a time asymptotic value (see right frame in Fig. 1), both pump and sideband are characterized by complex radial structures on intermediate scales between fast nonlinear oscillations on $\approx \bar{\gamma}_d^{-1/2}$ and the size of the linearly unstable region $\approx \bar{\gamma}_{P0}^{1/2} L$. To adequately evaluate the drift-wave intensity $\bar{I}$, we have taken a further spatial average of its value to make the result reasonably independent of the averaging method itself. Figure 3 shows the results of the spatially averaged drift-wave intensity $\langle \bar{I} \rangle$ on 1/5 of the linearly unstable domain [13]. In the $L \to \infty$ limit, numerical results reflect well the values for the fluctuation intensity expected from the fixed point solution, i.e., $\langle \bar{I}_f \rangle \simeq 0.15, 0.18, 0.23$, respectively, for $A = 1.15, 1.2, 1.3$. The scaling of $\langle \bar{I} \rangle$ with the system size is evident: it sharply increases with L for $L < 30$, suggesting a Bohm-like scaling of anomalous transport, and it eventually reaches the asymptotic value set by the fixed point solution for $L > 100$, where gyro-Bohm scaling is, indeed, expected. Because of the

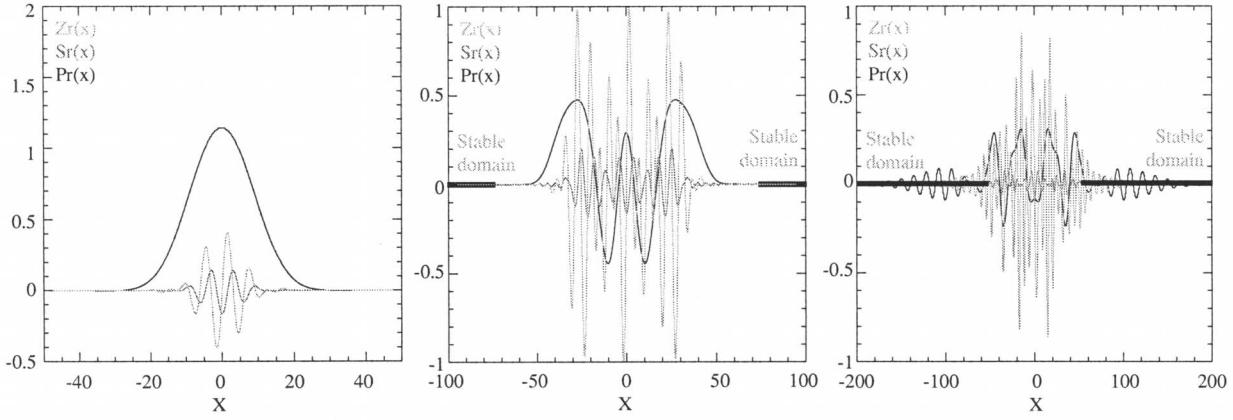

FIG. 1. Radial structure of the real part of the wave fields, ReP (black), ReS (red), and ReZ (green), at three subsequent times $\tau = 20$ (left), $\tau = 50$ (center), and $\tau = 125$ (right), for $A = 1.15$ and $L = 200$. The radial domain where the pump is linearly stable is also indicated.

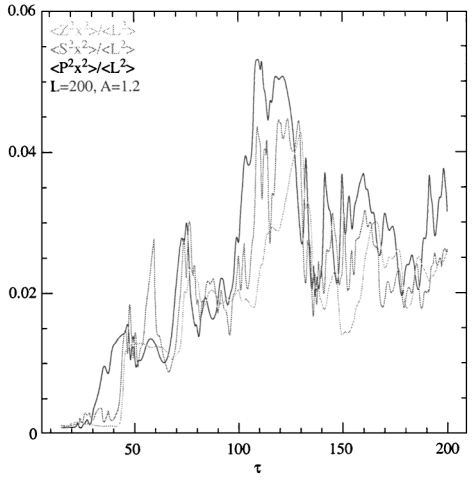

FIG. 2. Characteristic squared width of the wave fields normalized to L^2 as a function of time, for $A = 1.2$ and $L = 200$. Color code is the same as in Fig. 1.

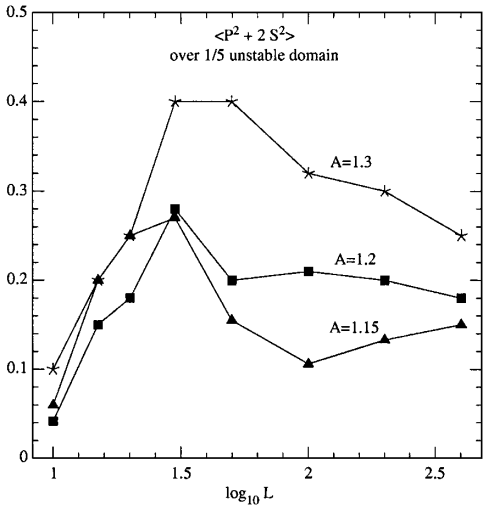

FIG. 3. Drift wave intensity $\langle \bar{I} \rangle$ vs L after spatial averaging on one-fifth of the linearly unstable domain. The three curves refer to $A = 1.15$, $A = 1.2$, and $A = 1.3$.

definition of $L = nq(\rho_i/r)(|s|/\rho_*)\Gamma^{-1/2}$, values obtained from simulation results depend intrinsically on dimensionless physical parameters such as magnetic shear and normalized poloidal wavelength. With the parameters of global gyrokinetic simulations reported in Ref. [4], and defining a as the tokamak minor radius, the present results predict a Bohm-like to gyro-Bohm transition for $a/\rho_i > 420$ and saturation to gyro-Bohm transport for $a/\rho_i > 1400$, in remarkable agreement with the results therein [4].

In summary, we have demonstrated that the coherent four-wave drift wave-zonal flow modulation interaction model of Chen, Lin, and White [7] not only captures the essential features observed in global gyrokinetic simulations in the $\rho_i/L_p \to 0$ limit, but, by allowing nonuniform equilibrium, accounts as well for size scaling of drift-wave intensity and turbulent diffusion. This model sets a hierarchy among the relevant nonlinear interactions, making it possible to consistently derive equations for the slow space-time evolution of drift-wave radial envelope and zonal flow structures. In the present approach, transport is a microscopic process which is due to particle scattering in the ambient turbulence. The scattering rate is set by the wave-particle decorrelation time, due to the local parallel mode structure, and depends linearly on the turbulence intensity [6]. This theoretical prediction could be readily checked by experimental measurements. In turn, the local turbulence intensity depends on global equilibrium properties due to turbulence spreading [5], ultimately causing turbulent diffusion dependence on the system size. The predicted size scaling of drift-wave intensity is remarkably similar to that of global gyrokinetic simulations [4].

This work was partly done with the support of U.S. DOE Grant No. DE-FG03-93ER54271 and Contract No. DE-AC02-76-CH03073 to the University of California at Irvine and Princeton Plasma Physics Laboratory.

[1] J. Connor and J. Taylor, Nucl. Fusion **17**, 1047 (1979).
[2] R. Budny *et al.*, Phys. Plasmas **7**, 5038 (2000).
[3] G. McKee *et al.*, Nucl. Fusion **41**, 1235 (2001).
[4] Z. Lin *et al.*, Phys. Rev. Lett. **88**, 195004 (2002).
[5] Z. Lin *et al.*, in *Proceedings of the 19th IAEA Fusion Energy Conference, Lyon, France, 2002* (Japan Atomic Energy Research Institute, Tokai, 2003).
[6] F. Zonca, R. White, and L. Chen, "Non-linear Paradigm for Drift-Wave—Zonal Flow Interplay: Coherence, Chaos and Turbulence."
[7] L. Chen *et al.*, Phys. Plasmas **7**, 3129 (2000).
[8] L. Chen *et al.*, Nucl. Fusion **41**, 747 (2001).
[9] Y. Lee and J.V. Dam, in *Proceedings of the Finite-Beta Theory Workshop, Varenna, 1977*, edited by B. Coppi and W. Sadowskii (U.S. Department of Energy, Washington, DC, 1977), p. 93.
[10] E. Frieman and L. Chen, Phys. Fluids **25**, 502 (1982).
[11] A. Hasegawa and K. Mima, Phys. Rev. Lett. **39**, 205 (1977).
[12] F. Hinton and M. Rosenbluth, Plasma Phys. Controlled Fusion **41**, A653 (1999).
[13] Z. Lin (private communication).